MARINE MAGNETIC ANOMALIES

Introduction

This lecture is basically the development of the equations needed to compute the scalar magnetic field that would be recorded by a magnetometer towed behind a ship given a magnetic timescale, a spreading rate, and a skewness. A number of assumptions are made to simplify the mathematics. The intent is to first review the origin of natural remnant magnetism (NRM) to illustrate that the magnetized layer is thin compared with its horizontal dimension. Then the relevant differential equations are developed and solved under the ideal case of seafloor spreading at the north magnetic pole. This development highlights the fourier approach to the solution to linear partial differential equations. The same approach will be used to develop the Green's functions for heat flow, flexure, gravity, and elastic dislocation. For a more general development of the geomagnetic solution, see the reference by *Parker* [1973].

Crustal Magnetization at a Spreading Ridge

As magma is extruded at the ridge axis, its temperature falls below the Curie point and the uppermost part of the crust becomes magnetized in the direction of the present-day magnetic field. Figure 1 from *Kent et al.* [1993] illustrates the current model of crustal generation. Partial melt that forms by pressure-release in the uppermost mantle (~40 km depth) percolates to a depth of about 2000 m beneath the ridge where it accumulates to form a thin magma lens. Beneath the lens is a mush-zone develops into a 3500-m thick gabbro layer by some complicated ductile flow. Above the lens, sheeted dikes (~1400-thick) are injected into the widening crack at the ridge axis. Part of this volcanism is extruded into the seafloor as pillow basalts. The pillow basalts and sheeted dikes cool rapidly below the Curie temperature as cool seawater percolates to a depth of at least 2000 m. This process forms the basic crustal layers seen by reflection and refraction seismology methods.

The highest magnetization occurs in the extrusive layer 2A (Figure 2) although the

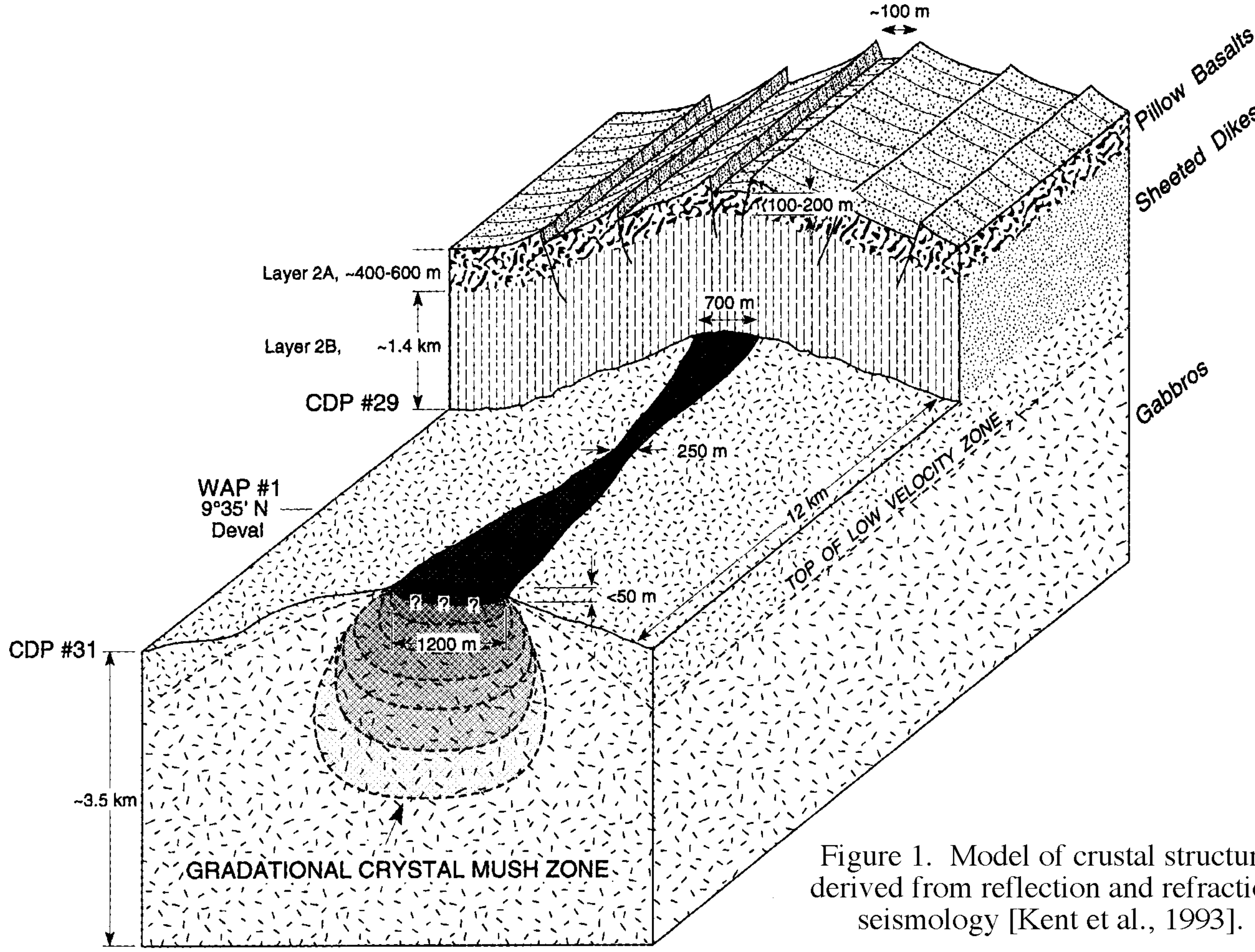

Figure 1. Model of crustal structure derived from reflection and refraction seismology [Kent et al., 1993].

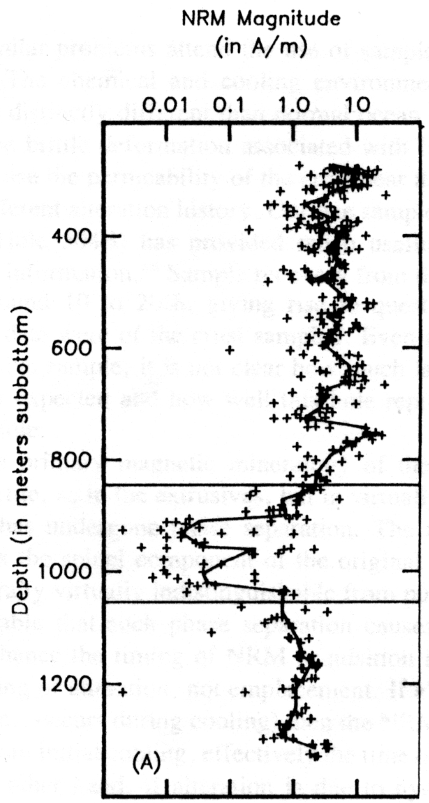

Figure 2. NRM values (in A/m) from Hole 504B. Depths are measured from the seabottom and include 274.5 m of sediment. The horizontal lines separate the upper units, transition zone, and dike complex. (From Smith, G. M. and Banerjee, S. K., *J. Geophys. Res.*, 91, 10337, 1986. With permission.)

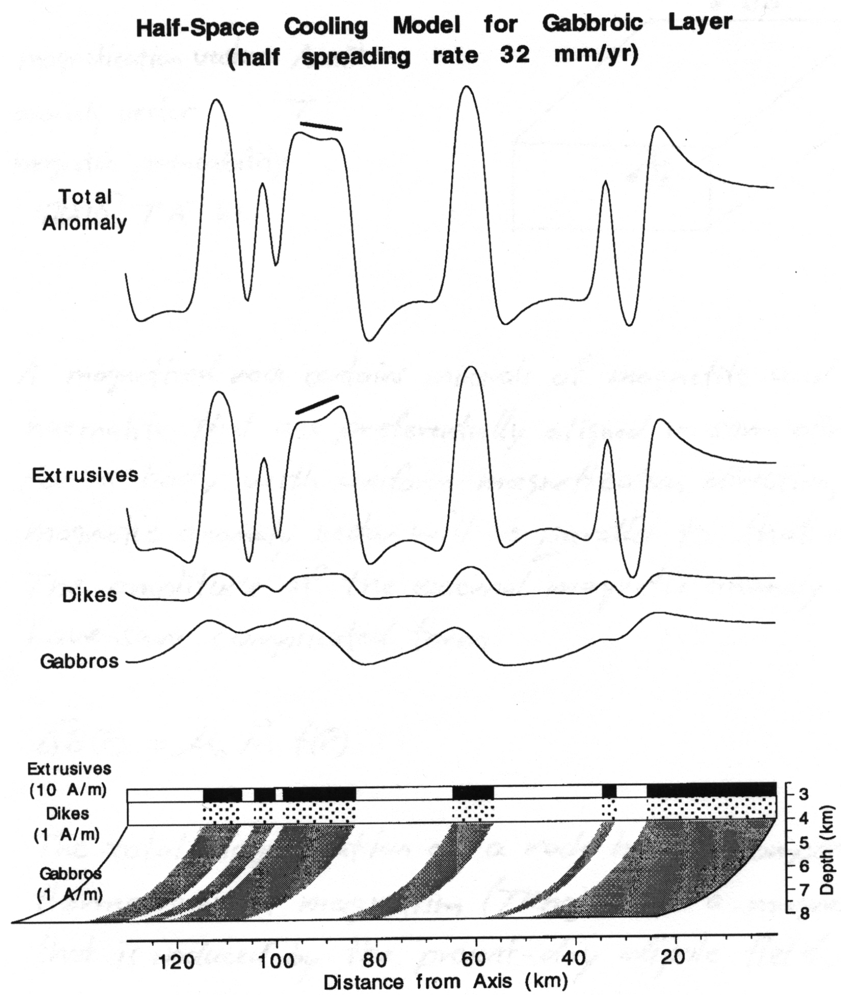

Figure 3 Magnetic anomalies generated by realistic model of crustal magnetization. The primary magnetization signature comes from the thin layer of extrusives. Dipping magnetization in te Gabbros reflects the position of the Curie isotherm at depth away from the ridge axis. (Jeff Gee, personal communication)

dikes and gabbro layers provide some contribution to the magnetic anomaly measured on the ocean surface. Note that the reversals recorded in the gabbro layer are do not have sharp vertical boundaries (Figure 3). The tilting reflects the time delay when the temperature of the gabbro falls below the Curie point. The sea-surface, magnetic-anomaly model shown in Figure 3 [*Gee and Kent*, 1994] includes the thickness and precise geometry of the magnetization of all three layers. For the calculation below, we assume all of the magnetic field comes from the thin extrusive layer.

Table - *Oceanic Crustal Structure and Magentization*

Layer	**Thickness/Velocity**	**Description**	**Thermoremnant Magnetism (TRM)**
layer 1	variable < 2.5 km/s	sediment	N/A
layer 2A	400 - 600 m 2.2 - 5.5 km/sec	extrusive, pillow basalts	5 - 10 A/m
magma lens			
layer 2B	1400 m 5.5 - 6.5 km/s	intrusive, sheeted dikes	~1 A/m
layer 3	3500 m 6.8 - 7.6km/s	intrusive, gabbro	~1 A/m

The other assumptions are the ridge axis is 2-D so there are no along-strike variations in magnetization and the spreading rate is uniform with time. Before going into the calculation, we briefly review the magnetic field generated by a uniformly magnetized block.

Uniformly Magnetized Block

M - magnetization vector (Am^{-1})
Δ **B** - magnetic anomaly vector (T)
μ_o - magnetic permeability ($4\pi \times 10^{-7}$ $TA^{-1}m$)

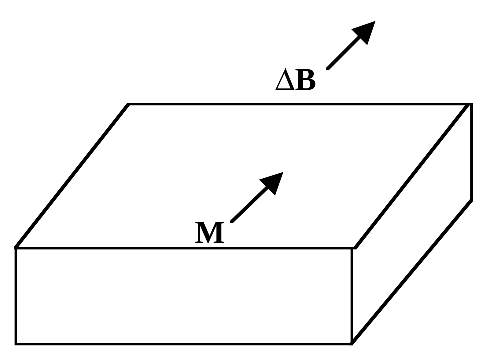

A magnetized rock contains minerals of magnetite and haematite that can be preferentially aligned in some direction. For a body with a uniform magnetization direction, the magnetic anomaly vector will be parallel to that direction. The amplitude of the external magnetic field will have some complicated form

$$\Delta\mathbf{B}(\mathbf{r}) = \mu_o \mathbf{M} f(\mathbf{r}) \tag{1}$$

where $f(\mathbf{r})$ is a function of position that depends on geometry. The total magnetization of a rock has two components, thermoremnant magnetism (TRM) $\mathbf{M}_{TRM}$ and magnetization that is induced by the present-day dipole field $\mathbf{M}_I$.

$$\mathbf{M} = \mathbf{M}_{TRM} + \mathbf{M}_I \qquad\qquad \mathbf{M}_I = \chi\mathbf{H} \tag{2}$$

where χ is the magnetic susceptibility and H is the applied dipole field of the Earth. The Koenigberger ratio Q is the ratio of the remnant field to the induced field. This value should be much greater than 1 to be able to detect the crustal anomaly. Like the magnetization, the value of Q is between 5 and 10 in Layer 2A but falls to about one deeper in the crust.

Anomalies in the Earth's Magnetic Field

When a magnetometer is towed behind a ship one measures the total magnetic field $\mathbf{B}$ and must subtract out the reference earth magnetic $\mathbf{B}_e$ field to establish the magnetic amomaly $\Delta\mathbf{B}$.

$$\mathbf{B} = \mathbf{B}_e + \Delta\mathbf{B} \tag{3}$$

Most marine magnetometers measure the scalar magnetic field. This is an easier measurement because the orientation of the magnetometer does not need to be known. The total scalar magnetic field is

$$|\mathbf{B}| = \left(|\mathbf{B}_e|^2 + 2\mathbf{B}_e \bullet \Delta\mathbf{B} + |\Delta\mathbf{B}|^2\right)^{1/2} \tag{4}$$

The dipolar field of the earth is typically 50,000 nT while the crustal anomalies are only about 300 nT. Thus $|\Delta\mathbf{B}|^2$ is small relative to the other terms and we can develop an approximate formula for the total scalar field.

$$|\mathbf{B}| \cong |\mathbf{B}_e|\left(1+\frac{2\Delta\mathbf{B}\bullet\mathbf{B}_e}{|\mathbf{B}_e|^2}\right)^{1/2} \quad \cong \quad |\mathbf{B}_e|\left(1+\frac{\Delta\mathbf{B}\bullet\mathbf{B}_e}{|\mathbf{B}_e|^2}\right) \tag{5}$$

Equation (5) can be re-arranged to relate the measured scalar anomaly $\mathbf{A}$ to the vector anomaly $\Delta\mathbf{B}$ given an independent measurement of the dipolar field of the earth $\mathbf{B}_e$.

$$\mathbf{A} = |\mathbf{B}| - |\mathbf{B}_e| = \frac{\Delta\mathbf{B}\bullet\mathbf{B}_e}{|\mathbf{B}_e|} \tag{6}$$

Magnetic Anomalies due to Seafloor Spreading

To calculate the anomalous scalar field on the sea surface due to thin magnetic stripes on the seafloor, we go back Poisson's equation relating magnetic field to magnetization. The model is shown in the following diagram. We have an *xyz* co-ordinate system with *z* pointed upward. The *z*=0 level corresponds to sea level and there is a thin magnetized layer at a depth of z_o.

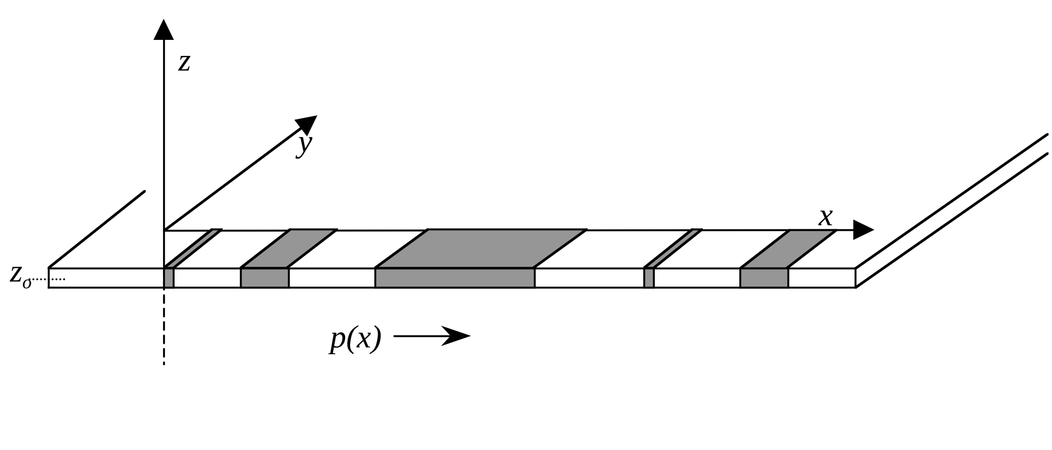

We define a scalar potential U and a magnetization vector **M**. The magnetic anomaly $\Delta\mathbf{B}$ is the negative gradient of the potential. The potential satisfies Laplace's equation above the source layer and is satisfies Poisson's equation within the source layer.

$$\Delta\mathbf{B} = -\nabla U \tag{7}$$

$$\nabla^2 U = 0 \qquad z \neq z_o \tag{8}$$

$$\nabla^2 U = \mu_o \nabla \bullet \mathbf{M} \qquad z = z_o \tag{9}$$

$U(x,y,z)$	-	magnetic potential	Tm
μ_o	-	magnetic permeability	TA^{-1} m = $4\pi x10^{-7}$
M	-	magnetization vector	Am^{-1}

In addition to assuming the layer is infinitesimally thin, we assume that the magnetization direction is constant but that the magnetization varies in strength and polarity as specified by the reversal function $p(x)$. The approach to the solution is:

i) solve the differential equation and calculate the magnetic potential U at z=0.

i) calculate the magnetic anomaly vector $\Delta\mathbf{B}$.

iii) calculate the scalar magnetic field A = $(\Delta\mathbf{B} \bullet \mathbf{B}_e)/|\mathbf{B}_e|$.

Let the magnetization be of the following general form.

$$\mathbf{M}(x,y,z) = \left(M_x\hat{i} + M_y\hat{j} + M_z\hat{k}\right)p(x)\delta(z - z_o) \tag{10}$$

The differential equation (9) becomes

$$\frac{\partial^2 U}{\partial x^2} + \frac{\partial^2 U}{\partial y^2} + \frac{\partial^2 U}{\partial z^2} = \mu_o\left[\frac{\partial}{\partial x}M_x p(x)\delta() + \cancel{\frac{\partial}{\partial y}M_y p(x)\delta()} + \frac{\partial}{\partial z}M_z p(x)\delta()\right] \tag{11}$$

The y-source term vanishes because the source does not vary in the y-direction (i.e. the y-derivative is zero). Thus the component of magnetization that is parallel to the ridge axis does not produce any external magnetic potential or external magnetic field. Consider a

N-S oriented spreading ridge at the magnetic equator. In this case the TRM of the crust has a component parallel to the dipole field which happens to be parallel to the ridge axis so there will be **no external magnetic field anomaly**.

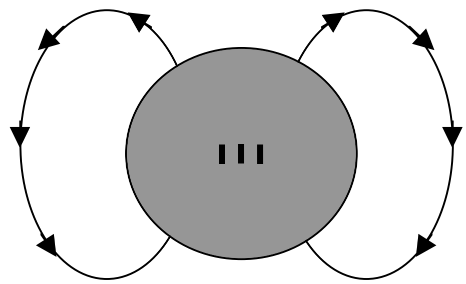

This explains why the global map of magnetic anomaly picks [*Cande et al.,* 1989] has no data in the equatorial Atlantic or the equatorial Pacific where ridges are oriented N-S. Now with the ridge-parallel component of magnetization gone, the differential equation reduces to.

$$\frac{\partial^2 U}{\partial x^2} + \frac{\partial^2 U}{\partial z^2} = \mu_o \left[\frac{\partial}{\partial x} M_x p(x) \delta(z - z_o) + \frac{\partial}{\partial z} M_z p(x) \delta(z - z_o) \right] \qquad (12)$$

This is a second order differential equation in 2 dimensions so 4 boundary conditions are needed for a unique solution.

$$\lim_{|x| \to \infty} U(\mathbf{x}) = 0 \quad \text{and} \quad \lim_{|z| \to \infty} U(\mathbf{x}) = 0 \qquad (13)$$

Take the 2-dimensional fourier transform of the differential equation where the forward and inverse transforms are defined as

$$F(\mathbf{k}) = \int_{-\infty}^{\infty}\int_{-\infty}^{\infty} f(\mathbf{x}) e^{-i2\pi(\mathbf{k}\cdot\mathbf{x})} d^2\mathbf{x} \qquad F(\mathbf{k}) = \Im_2[f(\mathbf{x})]$$

$$f(\mathbf{x}) = \int_{-\infty}^{\infty}\int_{-\infty}^{\infty} F(\mathbf{k}) e^{i2\pi(\mathbf{k}\cdot\mathbf{x})} d^2\mathbf{k} \qquad f(\mathbf{x}) = \Im_2^{-1}[F(\mathbf{k})] \qquad (14)$$

where $\mathbf{x} = (x, z)$ is the position vector, $\mathbf{k} = (k_x, k_z)$ is the wavenumber vector, and $(\mathbf{k} \bullet \mathbf{x}) = k_x x + k_z z$. The derivative property is $\Im_2[dU/dx] = i2\pi k_x \Im_2[U]$. The fourier transform of the differential equation is.

$$-\left[(2\pi k_x)^2 + (2\pi k_z)^2\right]U(k_x, k_z) = \mu_o p(k_x) e^{-i2\pi k_z z_o}(i2\pi \mathbf{k} \bullet \mathbf{M}) \qquad (15)$$

The fourier transform in the z-direction was done using the following identity.

$$\int_{-\infty}^{\infty} \delta(z - z_o) e^{-i2\pi k_z z}\, dz \equiv e^{-i2\pi k_z z_o} \qquad (16)$$

Now we can solve for $U(\mathbf{k})$

$$U(\mathbf{k}) = \frac{-i\mu_o}{2\pi} p(k_x)(\mathbf{k} \bullet \mathbf{M}) \frac{e^{-i2\pi k_z z_o}}{\left(k_x^2 + k_z^2\right)} \qquad (17)$$

Next, take the inverse fourier transform with respect to k_z using the Cauchy Residue Theorem (below).

$$U(k_x, z) = \frac{\mu_o}{2\pi i} p(k_x) \int_{-\infty}^{\infty} \frac{(\mathbf{k} \bullet \mathbf{M}) e^{i2\pi k_z (z - z_o)}}{\left(k_x^2 + k_z^2\right)} dk_z \qquad (18)$$

The poles of the integrand are found by factoring the denominator.

$$k_x^2 + k_z^2 = (k_z + ik_x)(k_z - ik_x) \qquad (19)$$

We see that $U(\mathbf{k})$ is an analytic function with poles at $\pm ik_x$. The integral of this function about any closed path in the complex k_z plane is zero unless the contour includes a pole in which case the integral is $i2\pi$ times the residue at the pole.

$$\oint \frac{f(z)}{z - z_o} dz = i2\pi f(z_o) \qquad (20)$$

One possible path integral is shown in the following diagram.

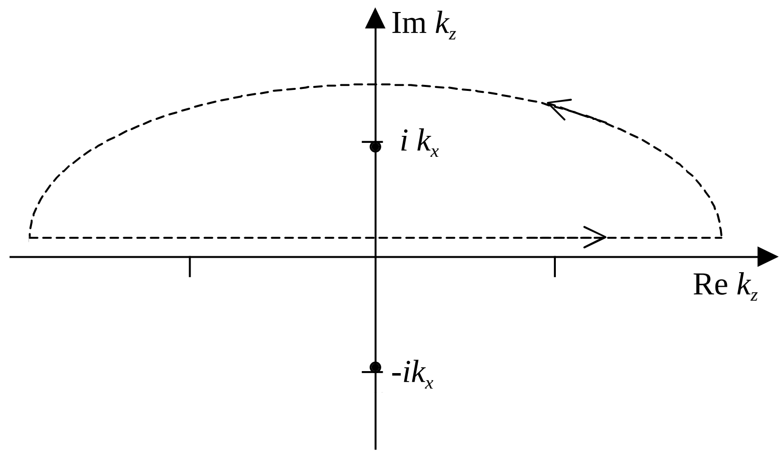

There are two ways to close the path at infinity. The selection of the proper path, and thus the residue, depends on the boundary condition, equation (13). First consider the case where $k_x > 0$. If we close the path of integration in the upper imaginary plane, then the pole will be ik_x. The residue will have an exponential term that vanished as z goes to plus infinity. This is what we need since the observation plane is above the source.

$$\oint ()dk_z = \frac{e^{-2\pi k_x(z-z_0)}}{2ik_x}\left(k_x M_x + ik_x M_z\right) \tag{20}$$

Next consider the case where $k_x < 0$. To satisfy the boundary condition as z goes to plus infinity, the $-ik_x$ pole should be used and the integration path will be clockwise instead of counterclockwise as in (20).

$$\oint ()dk_z = \frac{e^{+2\pi k_x(z-z_0)}}{2ik_x}\left(k_x M_x - ik_x M_z\right) \tag{21}$$

One can combine the two cases by using the absolute value of k_x

$$U(k,z) = \frac{\mu_0}{2} p(k) e^{-2\pi|k|(z-z_0)}\left(M_z - i\frac{k}{|k|}M_x\right) \tag{22}$$

where we have dropped the subscript on the x-wavenumber.

This is the general case of an infinitely-long ridge. To further simplify the problem, lets assume that this spreading ridge is located at the magnetic pole of the earth so the dipolar field lines will be parallel to the z-axis and there will be no x-component of magnetization. The result is.

$$U(k,z) = \frac{\mu_o M_z}{2} p(k) e^{-2\pi|k|(z-z_0)} \tag{23}$$

Next calculate the magnetic anomaly $\Delta\mathbf{B} = -\nabla U$.

$$\Delta\mathbf{B} = \left(-i2\pi k,\ 2\pi|k|\right) U(k,z) \tag{24}$$

The scalar magnetic field is given by equation (6) and since only the z-component of the earth's field is non-zero, the anomaly simplifies to.

$$\underset{\substack{\text{observed}\\\text{anomaly}}}{A(k,z)} = \underset{\substack{\text{reversal}\\\text{pattern}}}{\frac{\mu_o M_z}{2} p(k)} \times \underset{\substack{\text{earth}\\\text{filter}}}{2\pi|k| e^{-2\pi|k|(z-z_0)}} \tag{25}$$

The reversal pattern is a sequence of positive and negative polarities. To generate the model anomaly one would take the fourier transform of the reversal pattern, multiply by the *earth filter* and take the inverse transform of the result. An examination of the earth filter illustrates why a square-wave reversal pattern becomes distorted.

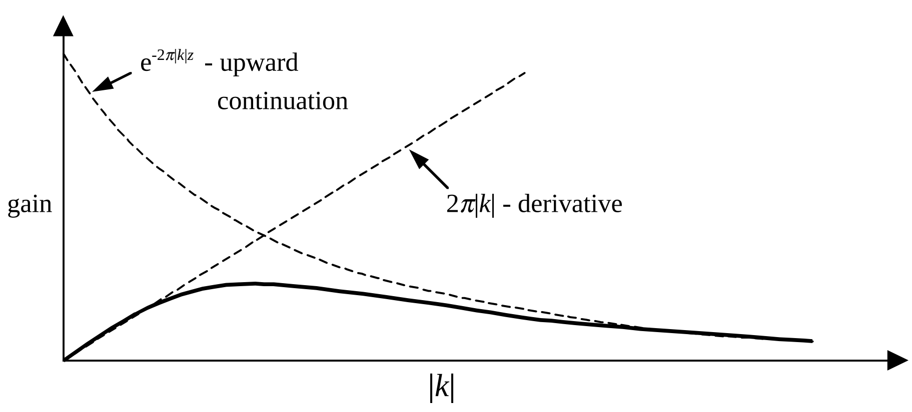

This earth filter attenuates both long and short wavelengths so it acts like a band-pass filter. In the space domain it modifies the shape of the square-wave reversal pattern as sketched in the following diagram.

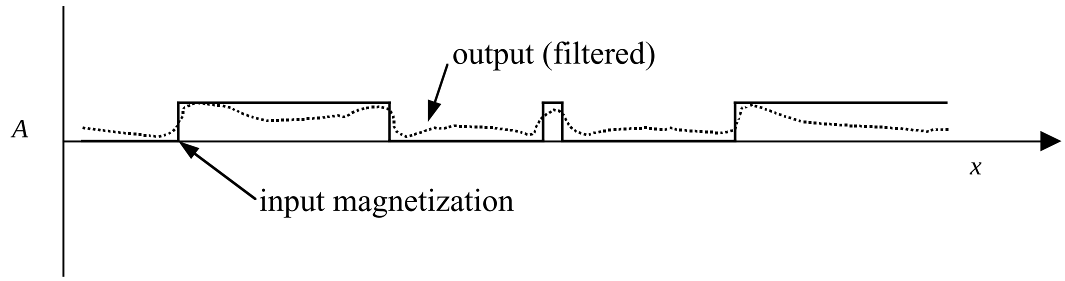

When the seafloor spreading ridge is not at the magnetic pole, both the magnetization and the earth's magnetic field will have an x-component. This introduces a phase shift or *skewness* Θ, in the output magnetic anomaly. At the ocean surface the skewed magnetic anomaly is.

$$A(k) = \frac{\mu_o M_z}{2} p(k) e^{i\Theta \frac{k}{|k|}} 2\pi|k| \mathrm{e}^{+2\pi|k|z_0} \qquad (26)$$

The skewness depends on both the geomagnetic latitude and the orientation of the spreading ridge when the crust was magnetized. Moreover, this parameter will vary over time. If one knows the skewness then the model profile can be skewed to match the observed profile. Alternatively, the observed magnetic anomaly can be de-skewed. This is called *reduction to the pole* because it synthesizes the anomaly that would have formed on the magnetic pole.

$$A_{pole}(k) = A_{observed}(k) e^{-i\Theta \frac{k}{|k|}} \qquad (27)$$

Discussion

The ability to observed magnetic reversals from a magnetometer towed behind a ship relies on some rather incredible coincidences related to reversal rate, spreading rate, ocean depth, and Earth temperatures, (mantle, seafloor, and Curie). In fact, the coincidence is so good that makes you wonder about "intelligent design"! In the case of marine magnetic anomalies, four scales must match.

First the temperature of the mantle (1200ßC), the seafloor (0ßC), and the Curie temperature of basalt (~500 ßC) must be just right for recording the direction of the Earth’s magnetic field at the seafloor spreading ridge axis. Most of the thermoremnant magnetism (TRM) is recorded in the upper 1000 meters of the oceanic crust. If the thickness of the TRM layer was too great, then as the plate cools while it moves off the spreading ridge axis, the positive and negative reversals would be juxtaposed in dipping vertical layers (Figure 3); this superposition would smear the pattern observed by a ship. If the seafloor temperature was above the Curie temperature, as it is on Venus, then no recording would be possible.

The second scale is related to ocean depth and thus the earth filter. The external magnetic field is the derivative of the magnetization which, as shown above, acts as a high-pass filter applied to the reversal pattern recorded in the crust. The magnetic field measured at the ocean surface will be naturally smooth (upward continuation) due to the distance from the seafloor to the sea surface; this is a low-pass filter. This smoothing depends exponentially on ocean depth so, for a wavelength of 2π times the mean ocean depth, the field amplitude will be attenuated by 1/e or 0.37 with respect to the value measured at the seafloor. The combined result of the derivative and the upward continuation is a band-pass filter with a peak response at a wavelength of 2π times the mean ocean depth or about 25-km. Wavelengths that are shorter (< 10 km) or much longer (> 500 km) than this value will be undetectable at the ocean surface.

The third and fourth scales that must match are the reversal rate and the seafloor-spreading rate. Half-spreading rates on the Earth vary from 10 to 80 km per million years. Thus for the magnetic anomalies to be most visible on the ocean surface, the reversal rate should be between 2.5 and 0.3 million years. It is astonishing that this is the typical reversal rate observed in sequences of lava flows on land!! While most ocean basins display clear reversal patterns, there was a period between 85 and 120 million years ago when the magnetic field polarity of the Earth remained positive so the ocean surface anomaly is too far from the reversal boundaries to provide timing information. This area of seafllor is called the Cretaceous Quiet Zone and it is a problem area for accurate plate reconstructions.

The lucky convergence of length and time scales makes it very unlikely that magnetic anomalies, due to crustal spreading, will ever be observed on the other planet. This is the main reason that I do not believe the recent publication that interprets the Martian field as ancient spreading anomalies - one cannot be this lucky twice!

References

Blakley, J., *Potential Theory in Gravity and Magentics*, Cambridge University Press, New York, 1995.

Cande, S.C., LaBrecque, J.L., Larson, R.L., Pitman, W.C., Golovchenko, X., and Haxby, W.F., 1989. *Magnetic Lineations of the World's Ocean Basins*. Tulsa, OK.

Phipps-Morgan, J., A. Harding, J. Orcutt, and Y.J. Chen, An Observational and Theoretical Synthesis of Magma Chamber Geometry and Crustal Genesis along a Mid-ocean Ridge Spreading Center, *in Magmatic Systems*, ed. M. P. Ryan, *Academic Press*, Inc., 1994. (Good review of crustal generation at mid-ocean ridges.)

Fowler, C.M.R., *The Solid Earth: An Introduction to Global Geophysics,* Cambridge University Press, 1990. (Marine magnetic anomalies and plate reconstructions - Chapter 3)

Gee, J and D. Kent, Variation in layer 2A thickness and the origin of the central anomaly magnetic high, *Geophys. Res., Lett., v. 21, no. 4*, 297-300, 1994.

Kent, G., A. Harding, J. Orcutt, Distribution of Magma Beneath the East Pacific Rise Between the Clipperton Transform and the 9ß17' Deval From Forward Modeling of Common Depth Point Data, *J. Geophys. Res., v. 98*, 13945-13969, 1993.

Pariso, J. E., and H. P. Johnson, Alteration processes at Deep Sea Drilling Project/Ocean Drilling Program Hole 504B at the Costa Rica Rift: Implications for magnetization of Oceanic Crust, *J. Geophys. Res., v. 96*, p. 11703-11722, 1991.

Parker, R. L., The rapid calculation of potential anomalies, *Geophys. J. Roy. Astr. Soc., v. 31*, p. 441-455, 1973. (**Required reading** for anyone interested in marine gravity/magnetics.)

Schouten, H. and McCamy, Filtering marine magnetic anomalies, *J. Geophys. Res., v. 77,* p. 7089-7099, 1972.

Turcotte, D. L. and Schubert, G., *Geodynamics: Applications of Continuum Physics to Geological Problems*, John Wiley & Sons, New York, 1982. (Plate tectonics - Chapter 1).